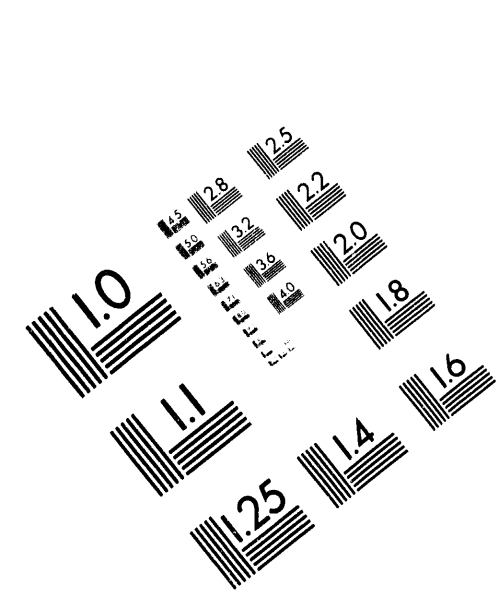

Association for Information and Image Management

1100 Wayne Avenue, Suite 1100
Silver Spring, Maryland 20910

301/587-8202

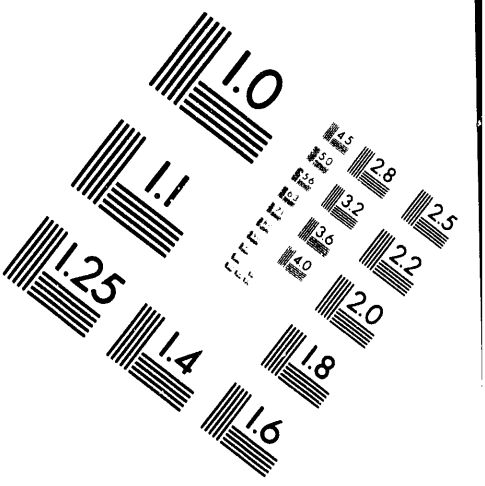

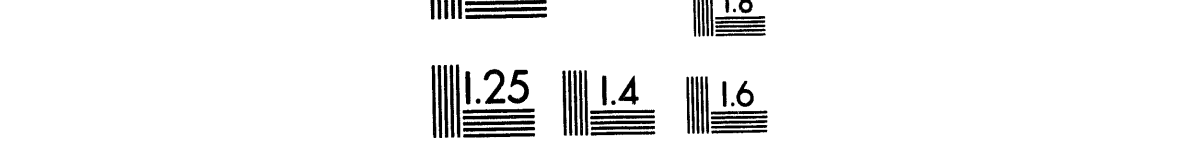

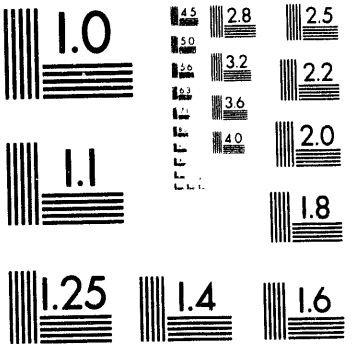

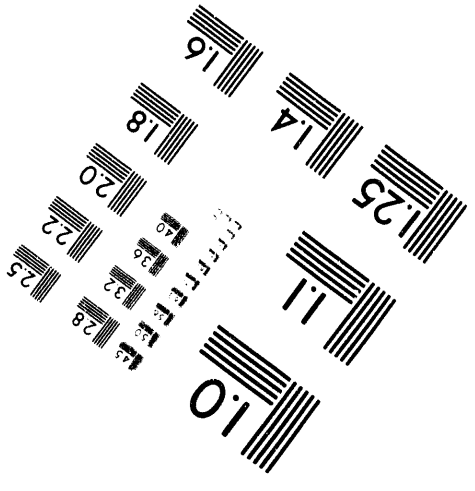

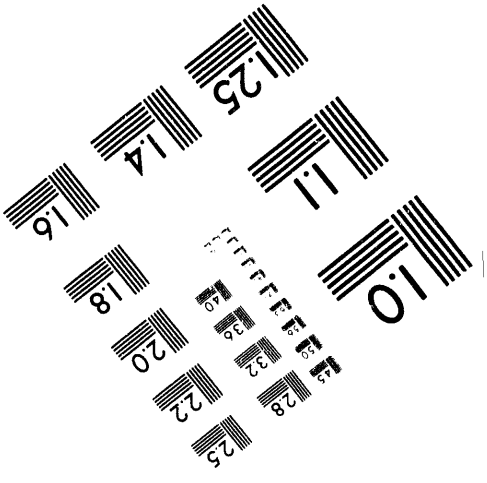

MANUFACTURED TO AIIM STANDARDS
BY APPLIED IMAGE, INC.

1 of 1

CONF-931009--28

TENSILE AND IMPACT PROPERTIES OF IRON-ALUMINUM ALLOYS*

D. J. Alexander and V. K. Sikka

Metals and Ceramics Division
OAK RIDGE NATIONAL LABORATORY
P.O. Box 2008
Oak Ridge, TN 37831-6151

---

*This research was sponsored by the U.S. Department of Energy, Fossil Energy AR&TD Materials Program (DOE/FE AA 15 10 10 0) under contract DE-AC05-84OR21400 with Martin Marietta Energy Systems, Inc.

The submitted manuscript has been authored by a contractor of the U.S. Government under contract No. DE-AC05-84OR21400. Accordingly, the U.S. Government retains a nonexclusive, royalty-free license to publish or reproduce the published form of this contribution, or allow others to do so, for U.S. Government purposes.

DISCLAIMER

This report was prepared as an account of work sponsored by an agency of the United States Government. Neither the United States Government nor any agency thereof, nor any of their employees, makes any warranty, express or implied, or assumes any legal liability or responsibility for the accuracy, completeness, or usefulness of any information, apparatus, product, or process disclosed, or represents that its use would not infringe privately owned rights. Reference herein to any specific commercial product, process, or service by trade name, trademark, manufacturer, or otherwise does not necessarily constitute or imply its endorsement, recommendation, or favoring by the United States Government or any agency thereof. The views and opinions of authors expressed herein do not necessarily state or reflect those of the United States Government or any agency thereof.

DISTRIBUTION OF THIS DOCUMENT IS UNLIMITED

TENSILE AND IMPACT PROPERTIES OF IRON-ALUMINUM ALLOYS

D. J. Alexander and V. K. Sikka

Metals and Ceramics Division
Oak Ridge National Laboratory
P.O. Box 2008
Oak Ridge, TN 37831-6151

Abstract

Tensile and impact tests have been conducted on specimens from a series of five heats of iron-aluminum alloys. These results have been compared to data for the iron aluminide alloy FA-129. The transition temperatures of all of the Fe_3Al-based alloys were similar, but the simple ternary alloy had a much higher upper-shelf energy. The reduced aluminum alloys [based on Fe-8Al (wt %)] had lower transition temperatures and higher upper-shelf energy levels than the Fe_3Al-type alloys. The reduced aluminum alloy with yttrium showed excellent tensile properties, with a room temperature total elongation of 40%, and a very high upper-shelf energy level. Despite the high tensile ductility at room temperature, the transition temperature of the yttrium-containing alloy was still about 150°C, compared to approximately 300°C for FA-129. In general, the microstructures were coarse and anisotropic. The fracture processes were dominated by second-phase particles.

Introduction

Iron-aluminum alloys based on the Fe_3Al iron aluminide offer an attractive combination of excellent corrosion and sulfidation resistance with low cost and acceptable strength. Work at Oak Ridge National Laboratory (ORNL) has resulted in significant improvements in the mechanical properties of these alloys. One of the candidate alloys has been designated FA-129 [1]. Although this alloy has potential for many applications, it can suffer from low ductility at room temperature due at least in part to environmentally induced embrittlement [2], and it has poor impact properties [3-5]. Recent work has shown that improvements in the tensile properties of iron-aluminum alloys can be achieved by reducing the aluminum content to about 8 wt % [6]. A series of alloys have been fabricated, and their tensile and impact properties have been measured for comparison to FA-129 data. This series of alloys contained several variants of Fe_3Al and several alloys with a reduced aluminum content.

Experimental Procedure

Five heats of material were prepared for comparison to results for the Fe_3Al alloy FA-129. The compositions of all of the alloys are given in Table 1. The FA-129 alloy contains chromium, niobium, and carbon additions. The simple ternary alloy was designed to match the aluminum and chromium levels of FA-129. A second alloy was made with the same composition but with zirconium and carbon additions, intended to provide some control of the grain size. Three more alloys were produced with a much lower level of aluminum, which would result in a disordered body-centered cubic (BCC) structure rather than the ordered B2 or DO_3 structure that the higher aluminum alloys would have. The FAP alloy matched the FA-129 chromium content, with a molybdenum addition for pitting resistance [6]. The FAP-Ti alloy contained titanium for grain size control. The FAP-Y alloy contained a yttrium addition intended to enhance the corrosion resistance of the alloy to compensate for its lower aluminum content [7].

The FA-129 material was vacuum-induction melted by Special Metals Corporation (New Hartford, New York) and cast into an ingot approximately 100 mm diam by 200 mm long. The ingot was processed at ORNL, with homogenization at 1150°C for 64 h, followed by 1 h at 700°C and air cooling. The material was heated to 1000°C for 2 h and extruded into bar roughly 25 by 75 mm. It was hot-rolled at 800°C to 19-mm

Table 1. Nominal Alloy Composition

Material	Heat number	Composition (wt %)						
		Al	Cr	Zr	Mo	C	Nb	Other
Fe_3Al alloys								
FA-129	D5-3966-1	15.9	5.5			0.05	1.0	
Ternary	14821	15.9	5.5					
Ter + Zr + C	14822	15.9	5.5	0.2		0.026		
Fe-8Al alloys								
FAP	14835	8.5	5.5	0.2	2.0	0.026		
FAP-Ti	14829	8.5	5.5	0.2	2.0	0.026		1.0 Ti
FAP-Y	14953	8.5	5.5	0.2	2.0	0.026		0.1 Y

thickness, and finish rolled at 650°C to a thickness of 16.5 mm. The other materials were fabricated and processed at ORNL. All of the alloys except the FAP-Y were vacuum-induction melted and cast into 72-mm-diam graphite molds. The ingots were hot extruded at 1000°C into bar 25 by 44 mm. The bars were hot forged at 800°C to 19-mm thickness, and then hot rolled at 650°C to 13 mm. They were reheated to 650°C and then flattened. The FAP-Y material was vacuum-induction melted and extruded into 15-mm-diam bar, annealed for 1 h at 800°C, and air cooled.

Charpy V-notch (CVN) specimens were machined and notched in the T-L orientation, so that crack extension was parallel to the rolling direction, except for the FAP-Y specimens which were taken along the length of the bar, so that crack extension was perpendicular to the extrusion direction. The specimens were heat treated after machining, the Fe_3Al-type alloys for 1 h at 700°C with either air cooling or an oil quench, and the reduced aluminum alloys for 1 h at 800°C with air cooling or an oil quench. The heat treatments will result in a structure that will be primarily B2 in the Fe_3Al-type alloys, while the reduced-aluminum alloys will have a disordered BCC structure. The FAP-Y specimens were not heat treated after machining.

The Charpy specimens were tested on a semiautomated impact test machine. Specimens tested above 300°C were heated in a small box furnace to the desired temperature, as indicated on a dummy specimen instrumented with thermocouples. When the test temperature was reached, the specimen was removed from the furnace, located on the anvils with the aid of specially designed tongs, and broken as quickly as possible (within 5 s). No estimate of the drop in temperature has been made, and the furnace temperature has been used as the test temperature.

Small tensile specimens were fabricated from the broken halves of the CVN specimens by electrodischarge machining. Therefore, all of the specimens were oriented perpendicular to the rolling direction, except for the FAP-Y specimens which were parallel to the extrusion direction. The specimens had a reduced section 1.78 × 2.54 × 6.35 mm long (0.070 × 0.100 × 0.250 in.) and were tested on a screw-driven electromechanical testing machine at a constant crosshead speed of 2.1×10^{-3} mm/s (0.005 in./min.) for an initial strain rate of 3×10^{-4} s^{-1}. High-temperature testing was conducted with a split-tube furnace, and temperature was monitored throughout the test with a thermocouple spotwelded on one end of the specimen. All tests were conducted in laboratory air.

Sections parallel and transverse to the rolling directions were metallographically polished and etched. The fracture surfaces of the tensile and CVN specimens were examined in a scanning electron microscope.

Results

Significant machining damage was noticed on many of the CVN specimens of the Fe_3Al-type materials. These cracks tended to be located on the faces of the specimens parallel to the original top and bottom of the plates, and were oriented perpendicular to the rolling direction. Many small cracks were also present at the base of the notches, parallel to the surfaces of the plates. Cracks were also evident on many of the machined tensile specimens, again for the Fe_3Al-type alloys. The reduced-aluminum alloys had much better finishes, and no evidence of cracking from the machining operations.

The results of the impact tests are shown in Fig. 1. The Fe_3Al alloys all showed similar behavior, with evidence of increased energy absorption only above about 200°C. The FA-129 and the ternary alloy with zirconium and carbon showed similar levels of energy absorption. The ternary alloy showed much higher energies from 400 to 600°C. Thus it is possible to achieve much higher levels of energy absorption with an Fe_3Al alloy than had been reached with FA-129. However, even slight alloying can greatly reduce the improvement. In general, the air-cooled specimens absorbed slightly more energy than the oil-quenched specimens, at higher test temperatures.

The reduced-aluminum alloys showed much higher levels of energy absorption than did FA-129, particularly the FAP-Y alloy. However, alloying additions in the FAP-Ti reduced the energy absorbed, as compared to FAP. Also, for these alloys the oil-quenched specimens were at least as good (FAP) or much better (FAP-Ti) than the air-cooled specimens. Two specimens of FAP-Ti were tested at 500°C, with very different

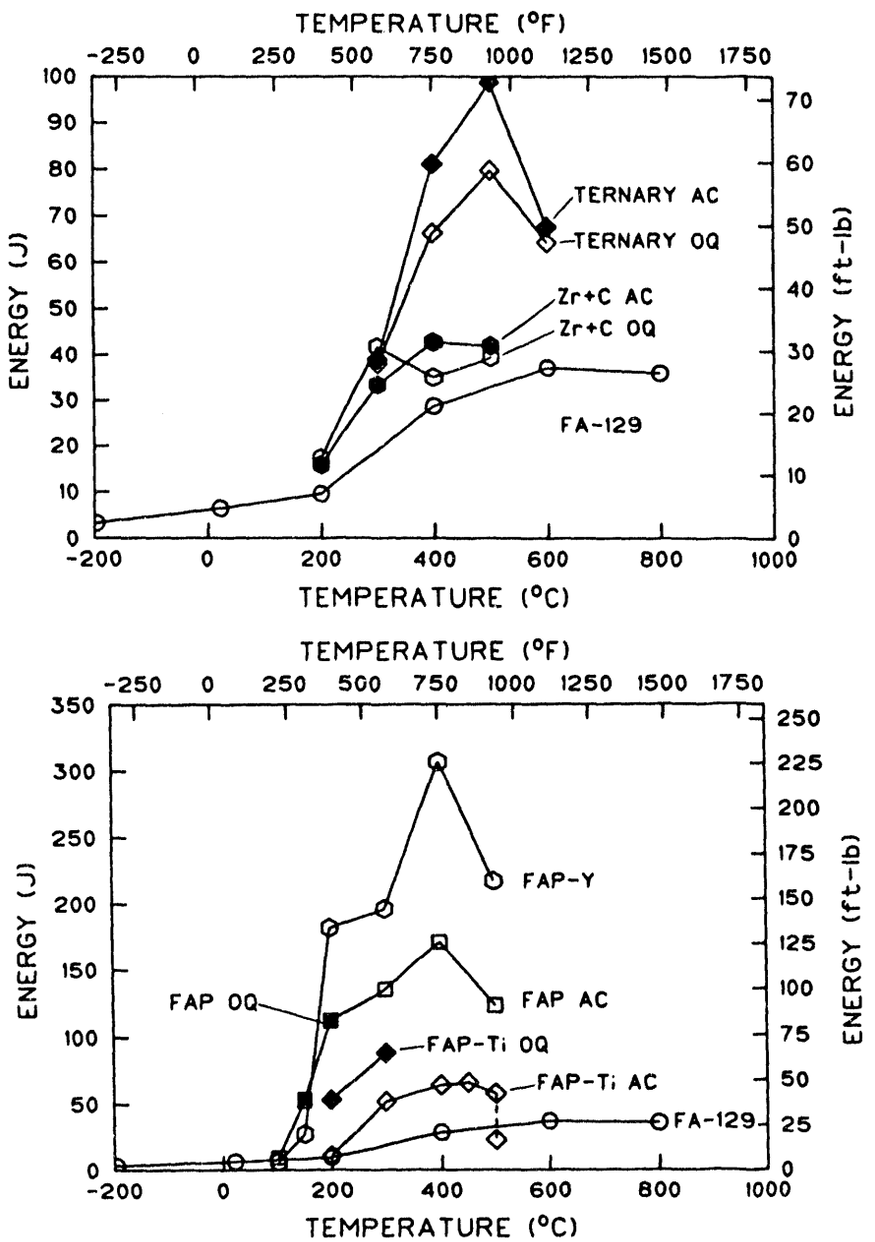

Fig. 1. Charpy impact tests for iron-aluminum alloys. Top: Fe_3Al-type alloys. Bottom: lower aluminum content alloys. Note the much higher upper-shelf energy levels of the FAP and FAP-Y alloys.

absorbed energies. It is believed that the lower level is not representative of the material, judging from the remainder of the specimens. The FAP-Y alloy had better properties than any of the other alloys, with an upper-shelf energy level of about 250 J, but the ductile-to-brittle transition temperature (DBTT) was still quite high, at around 150°C.

The tensile properties of the alloys are shown in Fig. 2, and summarized in Table 2. The simple ternary alloy was much weaker than the other alloys. The addition of zirconium and carbon increased the strength of the alloy significantly. In general, the FAP-type alloys had strengths similar to FA-129, with the FAP and FAP-Y alloys being slightly weaker and FAP-Ti slightly stronger than FA-129. All of the FAP-type alloys showed higher ductility than FA-129 and most of the Fe_3Al-type alloys. The FAP-Y alloy had 40% total elongation at room temperature, showing excellent ductility. The effect of the cooling rate noted for the CVN specimens was also apparent in the tensile results, with the oil-quenched FAP-Ti alloy showing much better ductility than the air-cooled FAP-Ti, just as the oil-quenched FAP-Ti had much better impact properties than the same air-cooled material.

Sections were taken parallel to the fracture surfaces from specimens of each alloy, and polished and etched for examination of the microstructures. These results are shown in Fig. 3. In general, the materials tended to be anisotropic, with a layered pancake structure. In addition, numerous second-phase particles were present. For many of the alloys processed by extrusion, a gradient existed from the surface to the center of the specimens, with finer grains near the surfaces and larger grains along the center. This suggests that the processing schedule was not optimized, as the processing was not able to produce a uniform deformation in the material that would have resulted in an equiaxed recrystallized structure.

The ternary alloy is shown in Fig. 3a. The grain size was very large, and some inclusions were visible in the matrix. The ternary alloy with zirconium and carbon, shown in Fig. 3b, had a much smaller grain size, but the structure was very anisotropic, with layered grains that extended in the rolling direction. Some inclusions were present in this alloy also. The FA-129 material had many second-phase particles present in the matrix (Fig. 3c). There appear to be two types of particles: clusters of globular particles that may result from the iron-niobium eutectic solidification (Fig. 3d), and isolated rod-shaped particles distributed throughout the matrix (Fig. 3e). The appearance of the second-phase particles seemed to depend on the plane of sectioning, with the rodlike particles most obvious on a section normal to the rolling direction.

The reduced aluminum alloys had more equiaxed microstructures. The FAP alloy showed a gradient in the microstructure, with equiaxed grains near the surface and elongated grains at the midplane (Fig. 3f). The FAP-Ti microstructure was similar (Fig. 3g). The FAP-Y material had a fine-grained, equiaxed structure (Fig. 3h). All materials contained second-phase particles strung out along the rolling or extrusion direction.

The fracture surfaces of selected specimens were examined in a scanning electron microscope. The fracture processes were dominated by the second phase particles. It appears that the particles are damaging in two ways: at low and intermediate temperatures they create cracks that can then propagate into the matrix, thus increasing the transition temperature, and at higher temperatures they initiate large voids very easily, thus decreasing the upper-shelf energy.

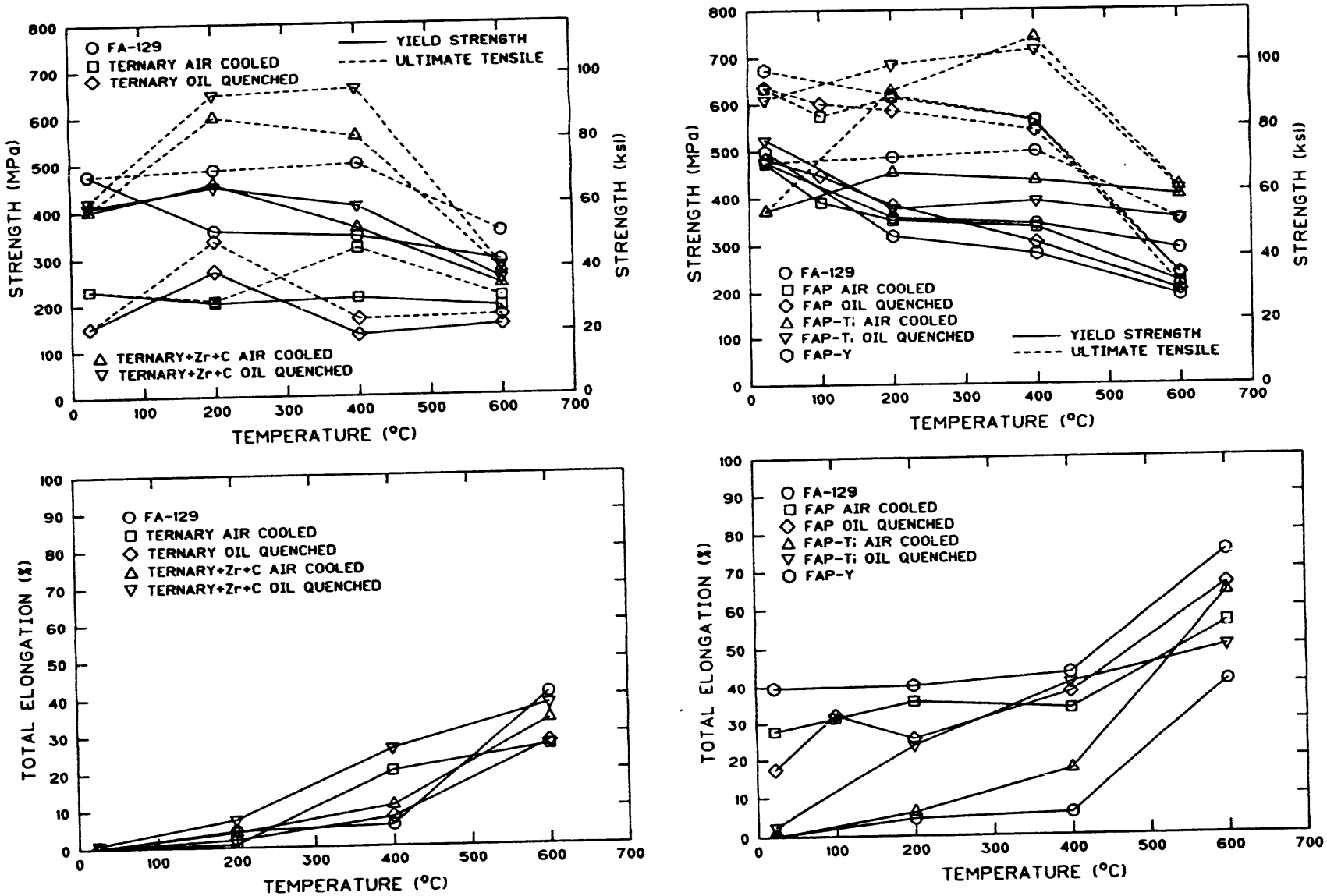

Fig. 2. Tensile properties of iron-aluminum alloys as a function of temperature. Top left: strength of Fe_3Al-type alloys. Top right: strength of low-aluminum content alloys. Bottom left: ductility of Fe_3Al-type alloys. Bottom right: ductility of low-aluminum content alloys.

Table 2. Tensile Properties of Iron-Aluminum Alloys

Alloy and heat treatment	Test temperature (°C)	Strength (MPa)		Total elongation (%)
		Yield	Ultimate tensile	
	Fe_3Al alloys			
FA-129	22	476	476	0
	200	357	486	4
	400	344	498	6
	600	291	352	41
Ternary air cooled	22	231	231	0
	200	203	208	1
	400	213	320	20
	600	190	213	27
Ternary oil quenched	22	150	150	0
	200	271	336	2
	400	133	167	8
	600	152	172	28
Ternary + Zr + C air cooled	22	401	401	0
	200	456	598	4
	400	361	558	11
	600	240	271	34
Ternary + Zr + C oil quenched	22	409	421	1
	200	451	647	7
	400	408	660	26
	600	251	279	38
	Fe-8Al alloys			
FAP air cooled	22	473	634	28
	100	390	574	31
	200	352	613	36
	400	337	563	34
	600	219	236	56
FAP oil quenched	22	482	637	17
	100	447	600	32
	200	383	585	25
	400	305	544	38
	600	203	239	66
FAP-Ti air cooled	22	372	372	0
	200	453	628	6
	400	435	741	17
	600	404	421	64
FAP-Ti oil quenched	22	525	610	2
	200	376	685	24
	400	392	714	41
	600	354	416	50
FAP-Y	22	499	675	40
	200	319	618	40
	400	281	564	43
	600	191	210	75

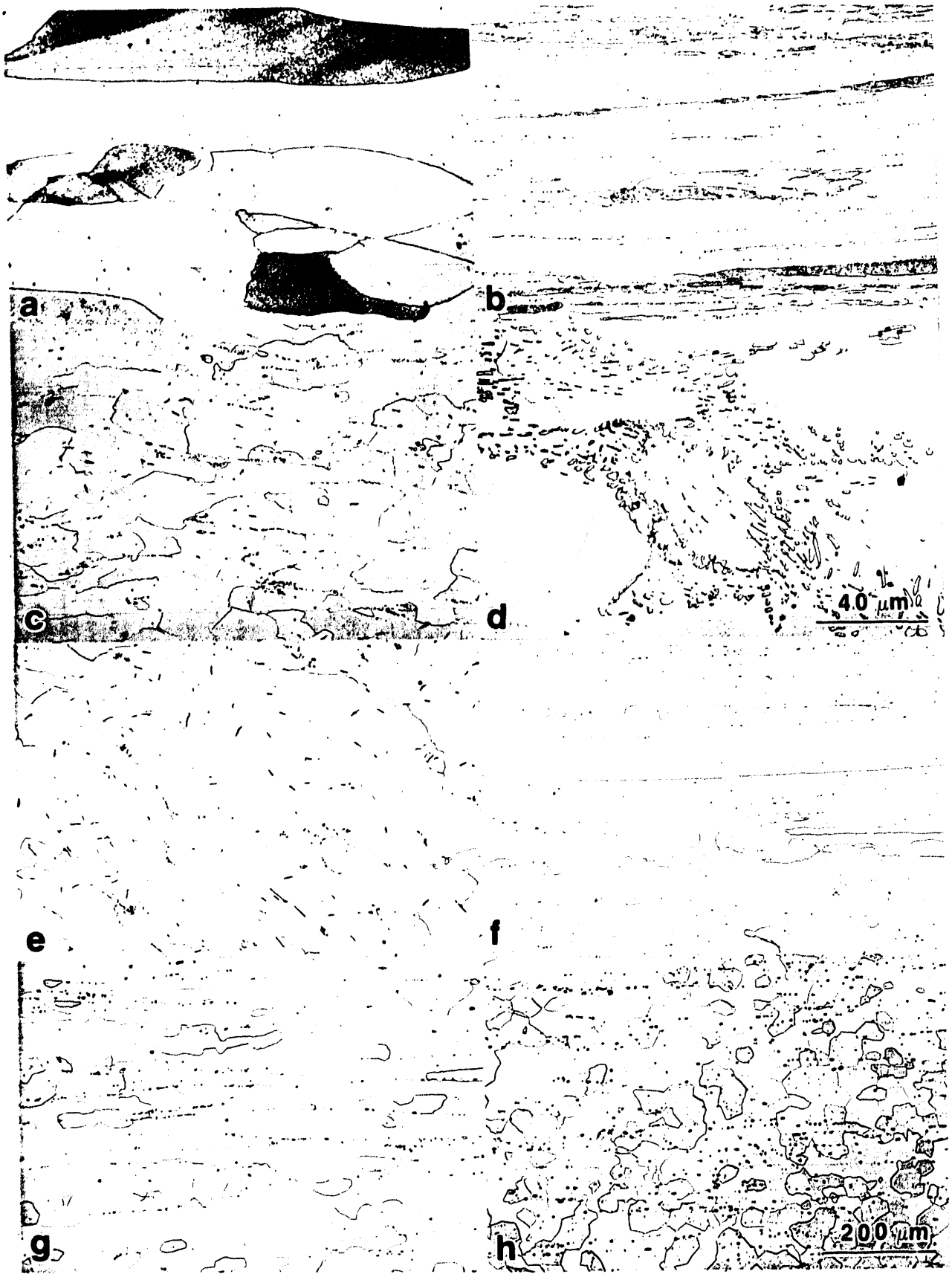

Fig. 3. Microstructures of the iron-aluminum alloys. a. Ternary alloy. b. Ternary plus zirconium and carbon. c. FA-129. d. Detail of clusters of particles in FA-129. e. Rod-like particles in FA-129. f. FAP near middle of thickness. g. FAP-Ti. h. FAP-Y. All photographs are at the same magnification except for Fig. 3d.

Fracture surfaces for FA-129 are shown in Fig. 4. At low temperatures the surface was predominantly cleavage fracture, although patches of intergranular fracture were present (Fig. 4a). Angular particles were often found at the cleavage initiation sites (Fig. 4b). At higher temperatures the fracture mode changed to quasicleavage, with more evidence of localized ductility in the fracture features. The large angular particles were again responsible for the fracture initiation (Fig. 4c). At the highest temperatures fracture occurred by microvoid coalescence (MVC), with large voids forming at the second-phase particles (Fig. 4d).

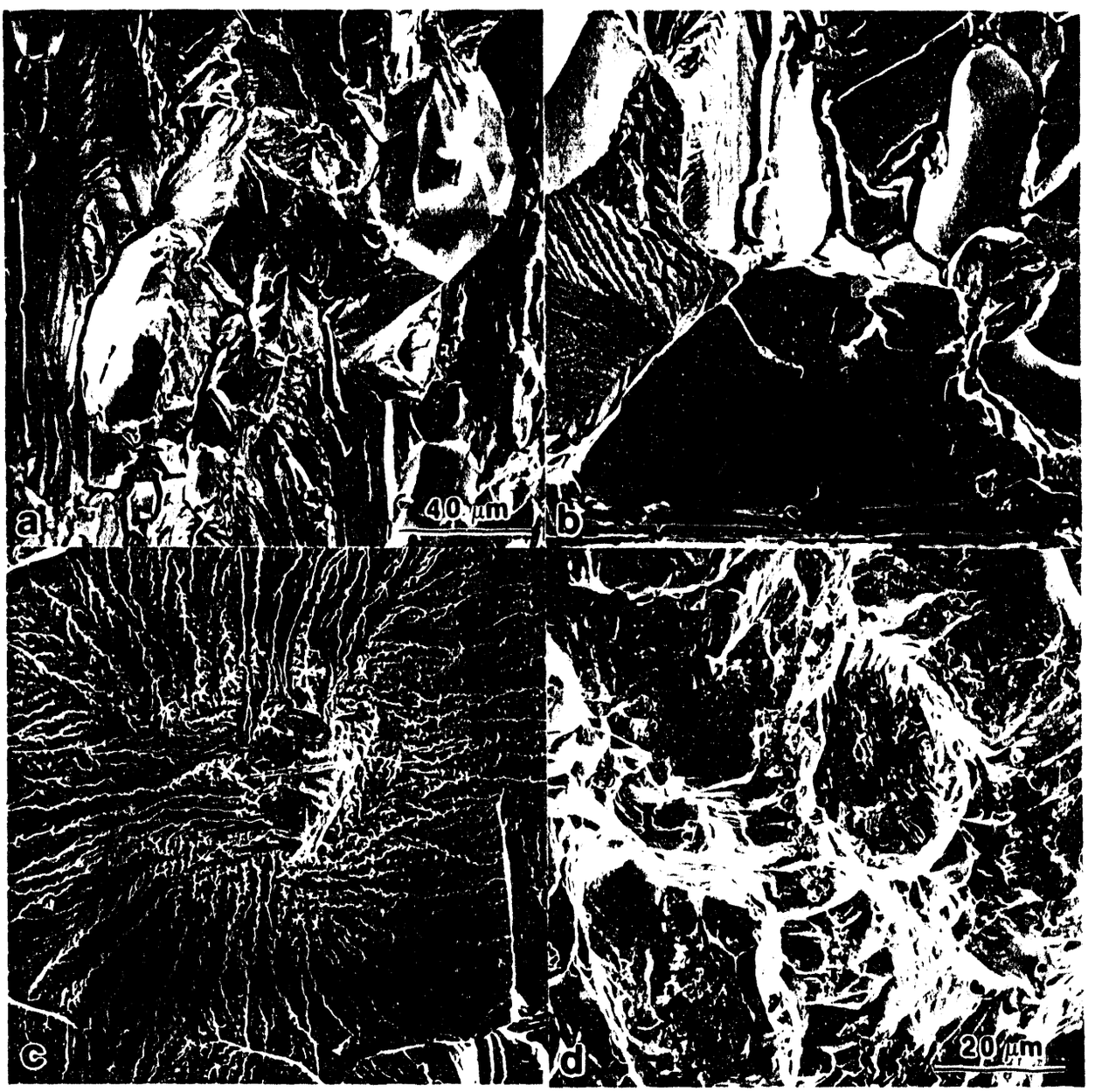

Fig. 4. Fracture surfaces from Charpy specimens of FA-129. a. Brittle fracture at 22°C. Some intergranular fracture is present with the cleavage fracture. b. Detail of an angular particle at the cleavage initiation site. c. Quasicleavage initiation site at 400°C. Note the angular particle at the center of the facet. d. Microvoid coalescence at 800°C. All photographs are at the same magnification except for Fig. 4a.

The ternary alloy had very large fracture facets, reflecting the very large grain size observed by optical metallography. At intermediate temperatures fracture began by a ductile process (Fig. 5a), but eventually transitioned to quasicleavage. No particles were associated with this transition. At higher temperatures fracture occurred by MVC (Fig. 5b), with small particles associated with the dimples. The ternary alloy with zirconium and carbon additions showed mostly cleavage and occasional intergranular fracture at low temperatures (Fig. 5c), and MVC at higher temperatures (Fig. 5d). Both of these alloys also showed intergranular splitting between the layers of the pancake structure.

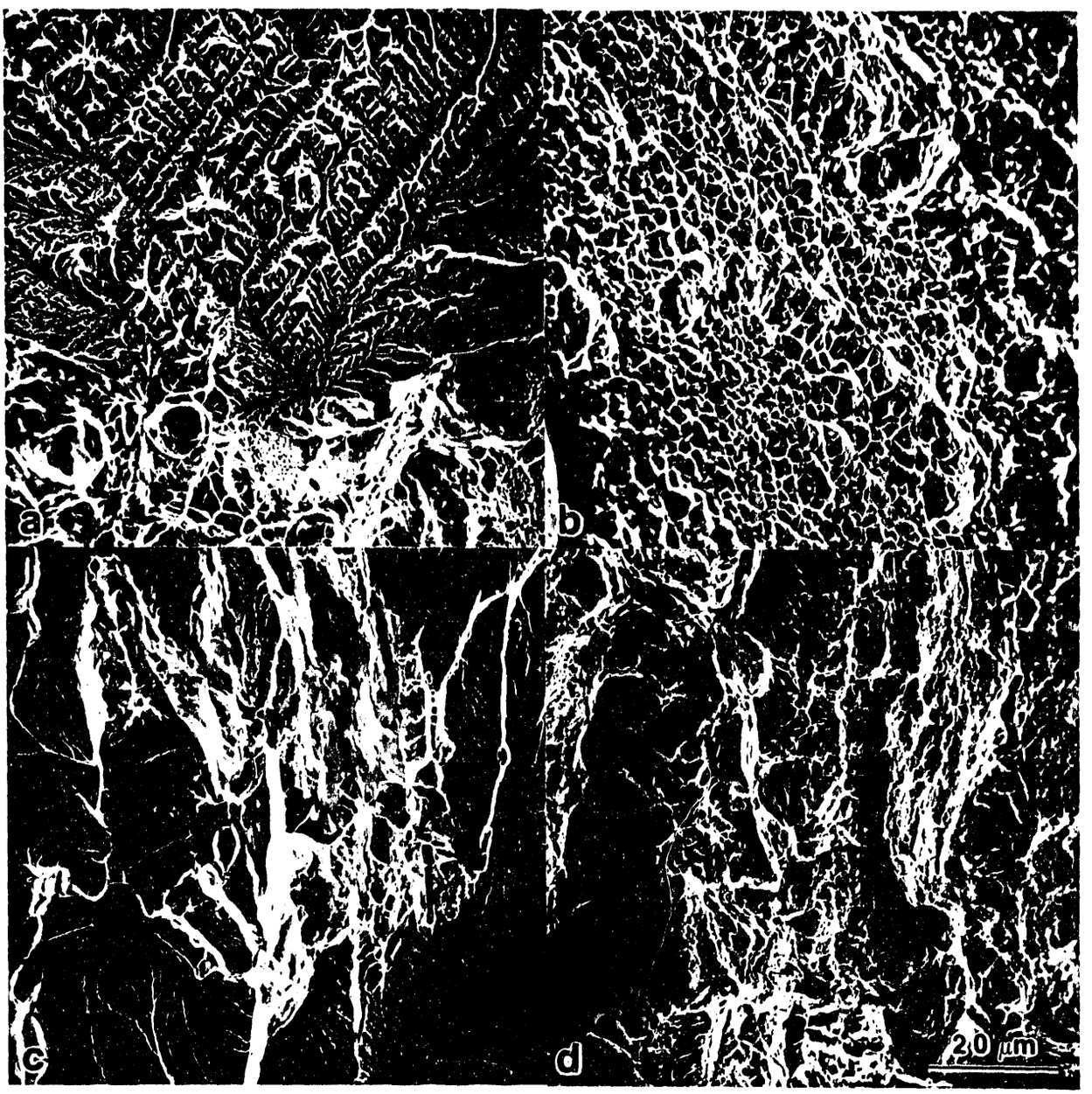

Fig. 5. Fracture surfaces from Charpy specimens of ternary and ternary plus Zr and C alloys. a. Ternary at 300°C. The quasicleavage pattern has an oriented appearance that probably reflects the local slip systems. b. Ternary at 500°C. c. Ternary plus Zr and C at 200°C. d. Ternary plus Zr and C at 400°C. All photographs are at the same magnification.

The FAP alloy also showed cleavage fracture at low temperatures (Fig. 6a), with the initiation sites again associated with second-phase particles. At high temperatures MVC fracture was again observed (Fig. 6b). The FAP-Ti alloy showed similar features (Figs. 6c and 6d).

The fractographic features for a FAP-Y Charpy specimen tested at 200°C are shown in Fig. 7. This specimen fractured initially by ductile tearing, with final fracture by cleavage. Regions of intergranular fracture are present, as was noted for many of the other alloys. Examination of the ductile fracture surface revealed the second-phase particles that were seen on the metallographic specimens (Fig. 7c).

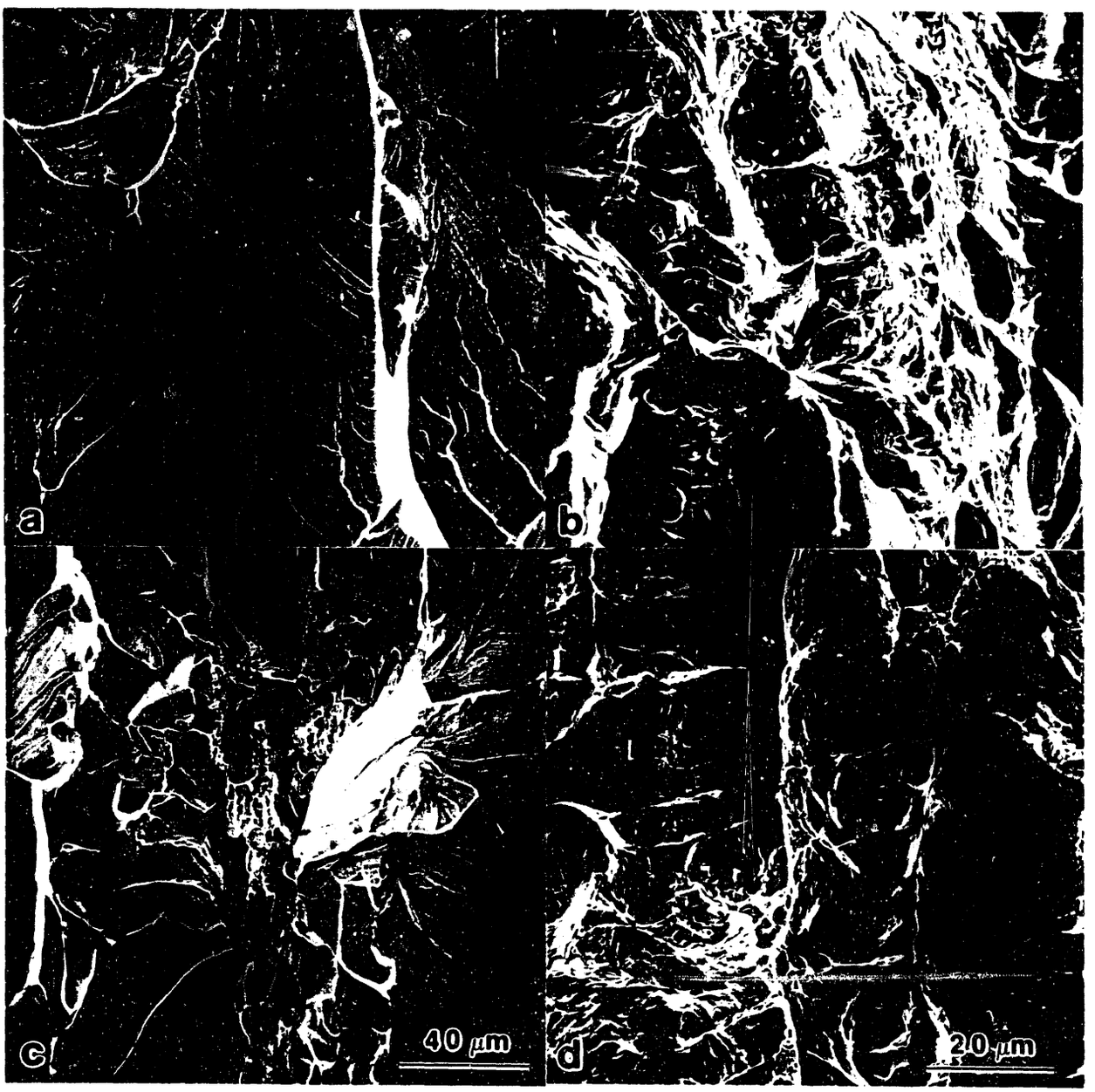

Fig. 6. Fracture surfaces from Charpy specimens of FAP and FAP-Ti alloys. a. FAP at 100°C; b. FAP at 200°C; c. FAP-Ti at 200°C; d. FAP-Ti at 400°C. All photographs are at the same magnification except for Fig. 6c.

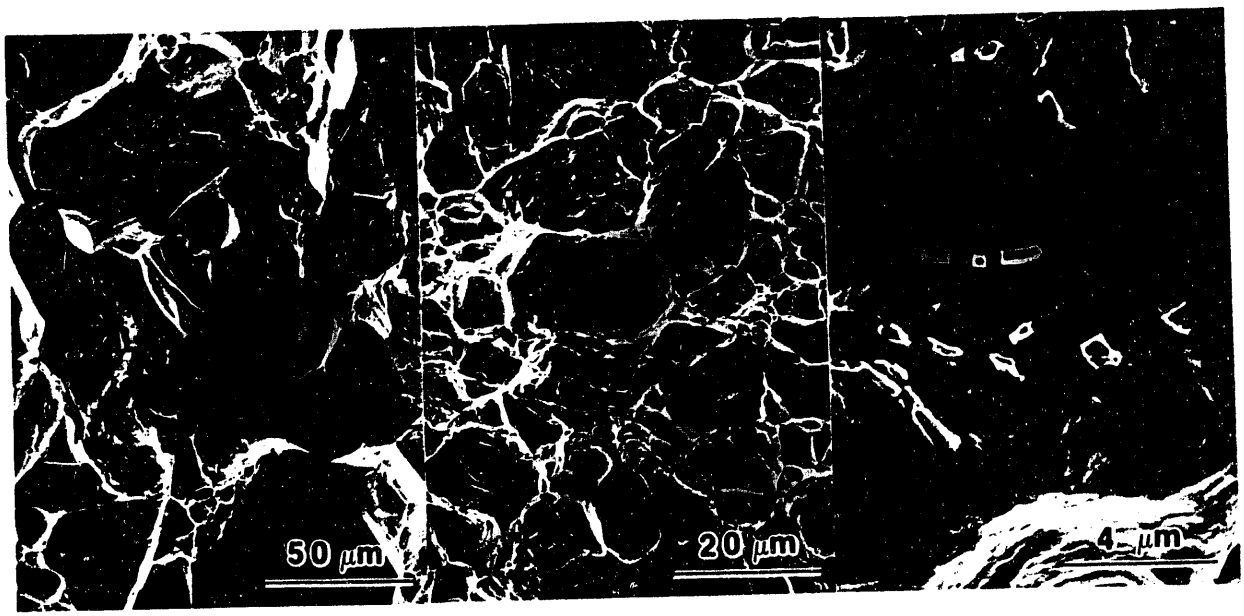

Fig. 7. Fractographic features from FAP-Y Charpy specimen tested at 200°C. Left: cleavage fracture, with regions of intergranular fracture. Middle: ductile microvoid coalescence. Right: detail of microvoids, showing particles associated with voids.

Discussion

The difficulties encountered in machining these iron aluminides are a serious problem. These alloys tend to be difficult to machine, and the large grain sizes probably exacerbate this problem. It is not clear whether the cracks were induced by the final grinding step or if they developed during earlier rough machining. The reduced aluminum alloys appear to be more machinable than the Fe_3Al alloys, but additional effort at understanding the problems with machining Fe_3Al alloys is needed.

The simple ternary alloy is much weaker than the other alloys. This is not surprising, since the material will not contain strengthening precipitates, and has a very coarse grain size. The addition of zirconium and carbon does refine the grains somewhat, and should also result in precipitates being formed. The result is much higher strength for the ternary plus zirconium and carbon alloy, as expected. The Fe_3Al-type alloys have very low ductility values, especially at the lower temperatures. In many cases, final fracture is coincident with initial yielding, with little or no plastic deformation, so the true yield strength may have been underestimated as a result of the premature fracture of the specimens.

The reduced aluminum alloys offer similar strength levels to FA-129, but with much greater ductility. This improvement has been attributed to a reduced susceptibility to environmental embrittlement as a result of the reduced aluminum content, since it is believed that the aluminum reacts with water vapor in the atmosphere to generate hydrogen that is responsible for the embrittlement [2,6]. In addition, dislocation movement should be much easier in the disordered BCC structure in the reduced aluminum alloys than in the ordered B2 structure in FA-129. This should also contribute to the increased ductility. The FAP-Y alloy should also benefit from its fine, equiaxed grain structure. It is not clear whether this is due to the yttrium addition or the processing procedures.

The impact properties of the Fe_3Al-type alloys are somewhat better than those of FA-129, but not dramatically so. The Fe_3Al-based alloys all have similar transition temperatures of about 250°C. The upper-shelf energies of the simple ternary alloy are greater than those of the other alloys, but even small alloying additions of zirconium and carbon reduce the upper shelf significantly. It is clear that the second-phase particles are dominating the fracture processes, although different particles may be involved in the different alloys, and at different temperatures. It seems unlikely that these coarse particles are beneficial to the strength of the materials, and so their removal seems an obvious step in improving the fracture resistance of these alloys. Microprobe analysis of the particles to determine at least their approximate composition would be very helpful in identifying either undesirable impurities or excessive alloying additions. Also, the deformation processing could be modified to produce a more equiaxed and isotropic structure of finer grains. This should improve both the strength and the transition behavior. A finer grain size might also improve the machinability of these materials.

The reduced aluminum alloys have better impact properties than the Fe_3Al alloys. The FAP alloy has a transition temperature of about 150°C, and a much greater upper-shelf energy than any of the Fe_3Al alloys. The FAP-Ti alloy has a transition temperature similar to the Fe_3Al alloys, but an upper-shelf energy that is better than that of FA-129. It seems that the disordered body-centered cubic structure of the reduced aluminum alloys is tougher than the ordered B2 structure of the Fe_3Al alloys. This is almost certainly the result of the easier motion of dislocations in the disordered structure. However, the addition of alloying elements and the subsequent presence of second-phase particles can degrade the impact properties, again showing the importance of second-phase particles to the fracture process.

The two classes of alloys show different responses to cooling rate. The Fe_3Al alloys show slightly better impact properties when they are air cooled, but the reduced aluminum alloys show similar or better properties when they are oil quenched. The effect for the FAP-Ti alloy is the most significant. In the Fe_3Al alloys the effects are minor, and no effect was observed for the FAP alloy. No differences between the air-cooled and the oil-quenched microstructures were apparent for any of the materials when examined by optical metallography. Microstructural changes due to the different cooling rates should be examined by transmission electron microscopy. Also, different cooling rates should be studied to determine if some other cooling rate could produce a further increase in the impact resistance.

An interesting feature of the impact properties is the maximum in the absorbed energy at intermediate temperatures. For the ternary alloy, the maximum energy is absorbed at 500°C, whereas the FAP alloy shows a maximum at 400°C. The reason for the drop in absorbed energy at higher temperatures is not known.

Many of the alloys show tendencies for intergranular fracture. It is unclear how greatly this contributes to the high transition temperatures, but it should be possible to suppress the formation of intergranular fracture by suitable alloying additions. Perhaps microalloying with boron would be effective in increasing the grain boundary cohesion for these alloys. The propensity for intergranular fracture may indicate that these alloys will be susceptible to further embrittlement on exposure to high temperatures, and this possibility should be examined.

The high DBTT for the FAP-Y of about 150°C is surprising, considering the excellent tensile properties present at room temperature. One possible explanation is that the alloy may be strain-rate sensitive. Recent work with thin sheet specimens of FAP-Y has indicated very little effect of strain rate on the yield strength of this alloy for strain rates from 10^{-6} to 10^{0} s^{-1} [8]. However, it seems likely that this material will exhibit strain-rate sensitivity at higher strain rates such as those associated with an impact test. Also, there may be some differences between the microstructures in the thick material and the thin sheet stock. Additional tests are planned to investigate these possibilities This alloy also shows a tendency for intergranular fracture, as do many of the other materials. This may contribute to the poor impact resistance, but since the brittle fracture surface is primarily cleavage, the intergranular fracture is not likely to play a major role.

Conclusions

A series of alloys have been made to investigate the tensile and impact properties of ordered Fe_3Al-based alloys and reduced-aluminum alloys with a disordered structure. The alloys tended to have coarse anisotropic microstructures, with many second-phase particles; these particles dominated the fracture process. In general, the reduced-aluminum alloys offer better ductility and higher upper-shelf energies than the Fe_3Al-type alloys. In particular, the FAP-Y alloy offers excellent tensile ductility at room temperature. However, all of the alloys suffer from high ductile-to brittle transition temperatures. Further improvements in the fracture properties should be possible by: refining the grain size; eliminating the second-phase particles; increasing the grain boundary cohesion to suppress intergranular fracture; optimizing the cooling rate; and adopting better machining practices. The best alloy, FAP-Y, has a DBTT of about 150°C, despite having 40% total elongation at room temperature. Further work is needed to determine the reasons for the surprisingly high transition temperature in this ductile material.

Acknowledgments

This research was sponsored by the U.S. Department of Energy, Fossil Energy AR&TD Materials Program (DOE/FE AA 15 10 10 0) under contract DE-AC05-84OR21400 with Martin Marietta Energy Systems, Inc. We would like to thank C. G. McKamey and S. Viswanathan for their helpful reviews of the manuscript, which was prepared by J. L. Bishop.

References

1. V. K. Sikka, C. G. McKamey, C. R. Howell, and R. H. Baldwin, "Fabrication and Mechanical Properties of Fe_3Al-Based Iron Aluminides," ORNL/TM-11465, Oak Ridge National Laboratory, Oak Ridge, TN, 1990.

2. C. T. Liu, C. G. McKamey, and E. H. Lee, "Environmental Effects on Room-Temperature Ductility and Fracture in Fe_3Al," Scripta Metall., 24 (1990), 385.

3. D. J. Alexander and V. K. Sikka, "Fracture Behavior of Fe_3Al Alloy FA-129," in Proceedings of the Fifth Annual Conference on Fossil Energy Materials, ORNL/FMP-1/1, Oak Ridge National Laboratory, Oak Ridge, TN, 1991, 239.

4. D. J. Alexander and V. K. Sikka, "Fracture of Iron Aluminide Alloys," in Proceedings of the Sixth Annual Conference on Fossil Energy Materials, ORNL/FMP-92/1, Oak Ridge National Laboratory, Oak Ridge, TN, 1992, 295.

5. B. G. Gieseke, D. J. Alexander, V. K. Sikka, and R. H. Baldwin, "Mechanical Properties of Ductile Fe_3Al-Based Plates," Scripta Metall. Mater., 29 (1993), 129-134.

6. V. K. Sikka, S. Viswanathan, and S. Vyas, "Acceptable Aluminum Additions for Minimal Environmental Effect in Iron-Aluminum Alloys," in High-Temperature Ordered Intermetallic Alloys V, I.Baker, R.Darolia, J. D. Whittenberger, and M. H. Yoo, eds., Mat. Res. Soc. Symp. Proc. Vol. 288, Materials Research Society, Pittsburgh, 1993, 971.

7. V. K. Sikka, S. Viswanathan, and C. G. McKamey, "Development and Commercialization Status of Fe_3Al-Based Intermetallic Alloys," in Structural Intermetallics, R. Darolia et al., eds., The Minerals, Metals and Materials Society, Warrendale, PA, 1993, 483.

8. V. K. Sikka, R. H. Baldwin, and C. R. Howell, "Low-Aluminum Content Iron-Aluminum Alloys," Proceedings of the Seventh Annual Conference on Fossil Energy Materials, ORNL/FMP-93/1, Oak Ridge National Laboratory, Oak Ridge, TN, 1993, 197.

DATE
FILMED
10/14/94

END